



## Original Research Article

# Preparation of Polymer Nanoparticles and Doping by Some Schiff Base Compounds by using Microemulsion Systems

Mohsin E. Aldokheily, Athraa H. Mekky, Soraj A. Rahem\*

Department of Chemistry, College of Science, University of Thi-Qar, Iraq

### ARTICLE INFO

#### Article history

Submitted: 2022-03-20

Revised: 2022-04-15

Accepted: 2022-04-17

Manuscript ID: CHEMM-2203-1459

Checked for Plagiarism: Yes

Language Editor:

Dr. Fatimah Ramezani

Editor who approved publication:

Professor Dr. Abdolkarim Zare

DOI:10.22034/CHEMM.2022.334829.1459

### KEYWORDS

Microemulsions

Nanoparticles

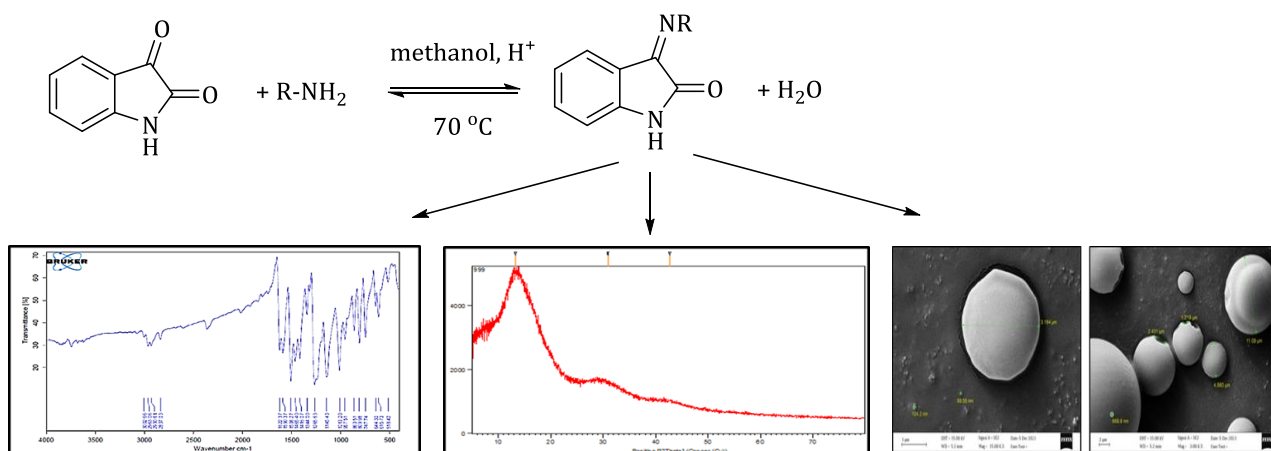
Schiff base

Doping

### ABSTRACT

This study aims to prepare the nanoparticles of polyacrylic polymer by emulsion method using inorganic phase water and organic phase chloroforms to mixture these phases by surfactant cetyltri methyl ammonium bromide (CTABr) and doping the polymer with Schiff base compounds to improve the properties of the polymer. The Schiff base from azomethene derivatives [A<sub>1</sub>-A<sub>2</sub>] have been synthesized from the reaction of isatin with hydrazine once and with ethyl-4-aminobenzoate one more time, however the Schiff base A<sub>3</sub> has been synthesized from 3,4-Dimethoxy benzylidene with hydrazine. The structures of polymer nanoparticles were identified by using X-Ray Diffractogram (XRD) to calculate crystallite sizes (D), and study the surface forms, morphology, and diameters of polymer nanoparticles by Scanning Electron Microscope (SEM) technology. In addition, the Infrared Spectroscopy (FT-IR) was utilized to characterize the functional groups of polyacrylic nanoparticle and Schiff base syntheses. Likewise, the Hydrogen-1 nuclear magnetic resonance spectroscopic (<sup>1</sup>H-NMR) and Carbon-13 nuclear magnetic resonance (<sup>13</sup>C-NMR) spectroscopic were used to determine Schiff base syntheses.

### GRAPHICAL ABSTRACT



\* Corresponding author: Soraj A. Rahem

✉ E-mail: [sorajalirahem91@gmail.com](mailto:sorajalirahem91@gmail.com)

© 2022 by SPC (Sami Publishing Company)

## Introduction

Microemulsions (MEs) are defined as the metastable colloidal dispersions consisting of two immiscible liquids that are isotropic transparent (or translucent) [1]. The internal (dispersed) phase is distributed in the form of small droplets in the external (continuous) phase, i.e. they form a heterogeneous mixture of the perfect dispersed droplets [2]. To form these droplets, the shear forces are necessary, which are usually applied by shaking, stirring, or sonication with surfactant addition [3].

Microemulsions are a special kind of emulsions which are of high significance due to the thermodynamic stability, the simplicity of manufacture, and high-solubility capacity for both lipophilic and hydrophilic compounds [4]. They are able to solubilize insoluble materials as polymers. [5] The term “polymer nano-composite” has evolved to refer to a multicomponent system in which the major constituent is a polymer or a blend thereof and the minor constituent has at least one dimension below 100 nm [6]. This study focused on the acrylic polymers nanoparticle properties and applications after doping with Schiff base compounds to improve the absorbing properties of the polymer.

The chemistry of Schiff base species has been initially of notable importance. Schiff bases also known as imine or azomethine [7]. They are organic compounds reactions between the substances containing amino groups ( $\text{NH}_2$ ,  $\text{NH}_2\text{OH}$ ,  $\text{NH}_2\text{-NH}_2$ , etc.) with carbonyl groups (aldehydes or some ketones) which in honor of the German chemist, Hugo Schiff, are called the Schiff base reactions [8]. The electrophilic carbon atoms of aldehydes and ketones can be the targets of nucleophilic attack by amines. The final result of this reaction is a compound in which the  $\text{C=O}$  double bond is replaced by a  $\text{C=N}$  double bond, and the general formula is  $\text{R}_1\text{R}_2\text{C=NR}_3$ , in which R is an organic side chain [9]. The Schiff bases are widely used for industrial purposes and also exhibit a broad range of biological activities [10].

## Materials and Methods

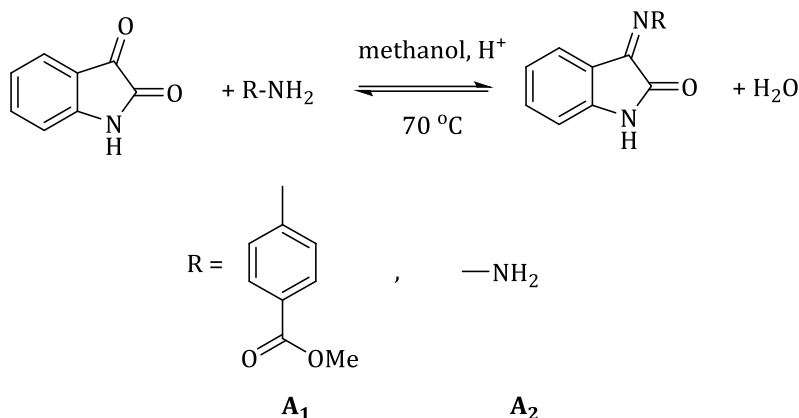
### Chemicals and Instrument

The primary substances and solvents in this study were purchased from BDH and Sigma Aldrich companies, which were used without further purification. The melting point was measured using a melting point apparatus and it was uncorrected. The Infrared spectroscopy (FT-IR) spectra were recorded by potassium bromide KBr disk on “Perkin Elme, tensor 27 Bruker” in the range of  $(400\text{-}4000)\text{ cm}^{-1}$  in the College of Science, University of Thi-Qar. Hydrogen-1 nuclear magnetic resonance ( $^1\text{H-NMR}$ ) and Carbon-13 nuclear magnetic resonance ( $^{13}\text{C-NMR}$ ) spectra were recorded on “a Bruker -DRX system Al 400 MHz spectrometer” solvent  $\text{d}_6\text{-DMSO}$  by the internal standard Tetramethyl silane (TMS) in Higher School of Chemistry/Sharif and Tehran Universities, Iran. The X-Ray Diffractogram (XRD) crystalline structure for any material can be recognized by studying the phase of (XRD) for that material, XRD Instrument, and Generator Settings 40 mA, 40 kV, Anode Material (Cu), Panalytical Company- MODEL X' Pert Pro, Iran. The Scanning Electron Microscope SEM type of the electron microscope captures the images of a sample by its scanning with a high-energy beam of the electron to produce signals which contain information about the sample's surface morphology, composition, etc. the FESEM instrument was ZEISS MODEL SIGMA VP, Iran.

### Preparation methods

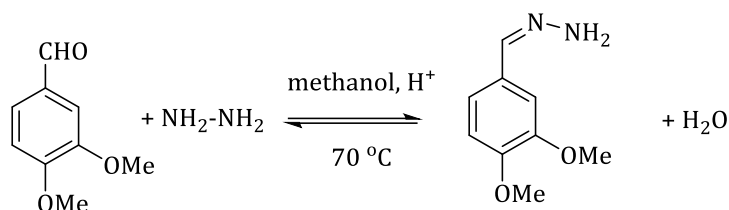
#### Synthesis of $A_1$ , $A_2$

Isatin 10 mmol (1.47 g) in 15 mL methanol was added to 0.1 mL of the glacial acetic acid, and 10 mmol (30 mmol) of ethyl-4-aminobenzoate, or hydrazine, respectively. The reaction mixture was refluxed for 24 hours, and then the solid product was filtered, dried, and recrystallized from ethanol to give  $A_1$  and  $A_2$ , respectively [11].

Scheme 1: Synthesis of A<sub>1</sub>, A<sub>2</sub>*Synthesis of A<sub>3</sub>*

3,4-Dimethoxy benzylidene (10 mmol, 1.66 g) in 15 mL methanol was added to 0.1 mL of the glacial

acetic acid, (10 mmol, 3200 mg) of hydrazine, and then the reaction mixture was refluxed for 12 hours. The solid product was filtered, dried, and recrystallized from ethanol to give A<sub>3</sub>.

Scheme 2: Synthesis of A<sub>3</sub>*Preparation of Polymer Nanoparticles*

The emulsion diffusion method was used to prepare polymer nanoparticles. First, chloroform (50 mL) and DI water (150 mL) were mixed by stirrer for 24 hours. Then, the mixture solvent was separated by a separator funnel to obtain the chloroform-saturated water and water-saturated chloroform, as well. The chloroform-saturated water was used to dissolve PCL 1.00 g and 0.03 g from the compounds of Schiff base synthesis, as indicated in Table 1. Next, the water-saturated chloroform was used to dissolve the surfactant CTABr 1.00 g. This organic phase was mixed and was kept with chloroform-saturated aqueous phase at 10-20 °C temperature. Then after, the stirrer (500) rpm was used for 1 h before being emulsified with an ultrasonic probe for 15 min. DI water (200 mL) was added to the reaction; while the moderate stirring was kept for 1 h. Finally, the chloroform and a part of water were removed using rotary evaporator under reducing pressure [12].

**Results and Discussion***Analysis of Schiff base (A<sub>1</sub>- A<sub>3</sub>)*

**Ethyl 4-[(3Z)-2-oxo-1,2-dihydro-3H-indol-3-ylidene]amino}benzoate A<sub>1</sub>**: Orange crystal, mp=230-233, Yield: 51% .

**FT-IR** (KBr, cm<sup>-1</sup>): 3187 (stretching of NH amide), 2985, 2906 (stretching of C-H<sub>aromatic</sub>), 2906 (stretching of C-H<sub>aliphatic</sub>), 1751 (C=O<sub>ester</sub>), 1655 (stretching of C=O<sub>amide</sub>), 1600 (stretching of C=N<sub>imine</sub>), 1336 (C-O), and 1352(C-N), as depicted in Figure S1 and Table 2.

**<sup>1</sup>H-NMR** (400 MHz, DMSO-d<sub>6</sub>) (δ ppm): 11.04 (s, 1H, NH), 8.06- 6.29 (m, 8H, aromatic protons) 4.31(q, 2H, OCH<sub>2</sub>CH<sub>3</sub>), 1.33 (t, 3H, OCH<sub>2</sub>CH<sub>3</sub>), and 2.5 of solvent (DMSO-d<sub>6</sub>), as demonstrated in Figure S2 and Table 3.

**<sup>13</sup>C-NMR** (101 MHz, DMSO-d<sub>6</sub>) (δ ppm) at 165.37 (C=O ester), 163.22 (C=O amide), 155.13 (C=N), 154.88- 111.69 (C=C aromatic), 60.74 O-CH<sub>2</sub>CH<sub>3</sub>, 14.26 CH<sub>2</sub>CH<sub>3</sub>, and 39.52 DMSO-d<sub>6</sub>, as presented in Figure S3 and Table 4.

**(3Z)-1H-indole-2,3-dione 3-hydrazone A<sub>2</sub>**: Yellow crystal, mp=168-170, Yield: 48%

**FT-IR** (KBr,  $\text{cm}^{-1}$ ): 3358, 3180 (stretching of  $\text{NH}_2$ ), 3157 (stretching of  $\text{NH}_{\text{amide}}$ ), 2957 (stretching of  $\text{C-H}_{\text{aromatic}}$ ), 1686 (stretching of  $\text{C=O}_{\text{amide}}$ ), and 1657 (stretching of  $\text{C=N}_{\text{imine}}$ ), as indicated in Figure S4 and Table 2.

**$^1\text{H-NMR}$**  (400 MHz,  $\text{DMSO-d}_6$ ) ( $\delta$  ppm): 10.70, 10.52 (s, 2H,  $\text{NH}_2$ ), 9.59 (s, 1H, NH of isatin), 7.36-6.84 (m, 4H for isatin ring), and 2.5  $\text{DMSO-d}_6$ , as depicted in Figure S5 and Table 3.

**$^{13}\text{C-NMR}$**  (101 MHz,  $\text{DMSO-d}_6$ ) ( $\delta$  ppm): 162.78 ( $\text{C=O}$ ), 138.64 ( $\text{C=N}$ ), 127.06-109.99, ( $\text{H-aromatic carbon}$ ), and 39.52  $\text{DMSO-d}_6$ , as indicated in Figure S6 and Table 4.

**3,4-dimethoxybenzaldehyde hydrazone  $\text{A}_3$** : Yellow crystal, mp=290-292, Yield: 82%.

**FT-IR** (KBr,  $\text{cm}^{-1}$ ): 3079 (stretching of  $\text{NH}_{\text{amide}}$ ), 3002, 2962 (stretching of  $\text{NH}_{\text{amine}}$ ), 3079 (stretching of  $\text{C-H}_{\text{aromatic}}$ ), 3002 (stretching of  $\text{C-H}_{\text{aliphatic}}$ ), 1623 (stretching of  $\text{C=O}_{\text{amide}}$ ), 1598 (stretching of  $\text{C=N}_{\text{imine}}$ ), 1344 ( $\text{C-O}$ ), and 1313 ( $\text{C-N}$ ), as illustrated in Figure S7 and Table 2.

**$^1\text{H-NMR}$**  (400 MHz,  $\text{DMSO-d}_6$ )  $\delta$  ppm: 8.64 (s, 1H, proton of imine), 7.49-7.38 (m, 3H, aromatic protons), 7.08 (s, 1H,  $\text{NH}_2$ ), 7.06 (s, 1H,  $\text{NH}_2$ ), 3.82 (s, 3H,  $\text{OCH}_3$ ), 3.35 (s, 3SH,  $\text{OCH}_3$ ) and 2.5  $\text{DMSO-d}_6$ , as presented in Figure 8 and Table 3.

**$^{13}\text{C-NMR}$**  (101 MHz,  $\text{DMSO-d}_6$ ) ( $\delta$  ppm) at 160.87, ( $\text{C=N}$ ), 151.60-108.96, ( $\text{C=C aromatic}$ ), 55.66, 55.42 ( $2\text{-O-CH}_3$ ), and 39.52 ( $\text{DMSO-d}_6$ ), as depicted in Figure S9 and Table 4.

#### Analysis of characterization of Polymer Nanoparticle

##### Analysis of Infrared Spectroscopy FT-IR

The FT-IR spectra of polymer polyacrylic in Figure S10 depicted bands at 2963, 2930, and  $2837\text{cm}^{-1}$  which were assigned to  $\text{C-H}_{\text{aliphatic}}$ . On the other hand, the band at  $1622\text{cm}^{-1}$  was owed to the stretching vibration of  $\text{C=O ester}$ .

In Figure S11, the FT-IR of  $\text{S}_1$  of the polymer doping with compound  $\text{A}_1$  demonstrated the absorption band at  $3017\text{cm}^{-1}$  which was designated to the stretching vibration of  $\text{C-H}_{\text{aromatic}}$ . The band at 2946, 2918, and  $2849\text{cm}^{-1}$  refers to  $\text{C-H aliphatic}$  and  $1590\text{cm}^{-1}$  to the  $\text{C=C}$  group. The absorption band at 1730 and  $1621\text{cm}^{-1}$  refers to  $\text{C=O}_{\text{ester}}$ ,  $\text{C=O}_{\text{amid}}$ , and 1640 to  $\text{C=N}$ ; while the bands

at 1274 and  $1243\text{cm}^{-1}$  referred to  $\text{C-N}$  and  $\text{C-O}$  [13].

While in Figure S12, the FT-IR spectra of  $\text{S}_2$  exhibited the following absorption bands at  $3014\text{cm}^{-1}$   $\text{C-H}_{\text{aromatic}}$ . The band at 2918 and  $2849\text{cm}^{-1}$  refers to the stretching vibration of  $\text{C-H polymer}$ . The absorption band at 1733 and  $1690\text{cm}^{-1}$  causes by stretching vibration of  $\text{C=O}_{\text{ester}}$ ,  $\text{C=O}_{\text{amid}}$ , and 1550 to  $\text{C=N}$ ; while bands at 1272 and  $1194\text{cm}^{-1}$  refer to  $\text{C-N}$  and  $\text{C-O}$ . In addition, the band at  $1436\text{cm}^{-1}$  refers to  $\text{N-N}$ .

On the other hand, FT-IR of  $\text{S}_3$  in Figure S13 indicated the absorption bands at  $3012\text{cm}^{-1}$  as being attributed to  $\text{C-H}_{\text{aromatic}}$ , and likewise the band at  $1570\text{cm}^{-1}$  refers to  $=\text{C-H}$  group. The band at  $2849\text{cm}^{-1}$  was due to the stretching vibration of  $-\text{C-H}$ . Besides, the bands at 1730 and  $1242\text{cm}^{-1}$  to  $\text{C=O}_{\text{ester}}$  and  $\text{C-O}$  groups, respectively. In addition, the stretching at  $1630\text{cm}^{-1}$  of  $\text{C=N}$ ,  $1391\text{cm}^{-1}$  of  $\text{N-N}$ , and  $1270\text{cm}^{-1}$  of  $\text{C-N}$  was presented in Table 5.

##### X-Ray Diffractogram Techniques (XRD)

The X-ray diffractogram (XRD) analysis has been performed to study the structure and crystallite size for the polymer doping by Schiff base synthesis in which the crystallite sizes are determined by Scherrer formula [14]:

$$D = \frac{K \lambda}{\beta \cos \theta}$$

Where  $K=0.89$  is the shape factor, ( $\lambda$ ) is the wavelength of irradiation ( $\text{Cu K}\alpha = 0.154056\text{nm}$ ),  $\beta$  is (FWHM), and  $\theta$  is XRD diffractogram angle, as indicated in Table 6.

According to the diffractogram of the pure acrylic polymer containing peaks at  $2\theta=13.2$ , its crystal size was 3.956 nm and a weak peak at  $2\theta=30.9$  and  $2\theta=42.7$  had 1.165, 2.110 nm crystal sizes, respectively which are depicted in Figure S14.

The XRD diffractogram is demonstrated in Figure S15 of the sample  $\text{S}_1$ , in which the highest peak at  $2\theta=21.467$  has height about 7360, and it has a peak at  $2\theta=20.47$  and its crystal sizes were about 39.229nm and 25.762nm, respectively. The second high peak at  $2\theta=24.513$  has height about 2331, and a peak at  $2\theta=24.01$  has crystal sizes about 36.516nm and 34.935nm, respectively which probably they return the density of peaks to

the factional groups from  $A_1$  in addition to the peaks of polymer nanoparticles [15].

The XRD diffractogram of sample  $S_2$  is presented in Figure S16 which indicates the highest peak at  $2\theta=21.459$  has height about 4990 and the crystal sizes 33.343nm, as well. It has a peak at  $2\theta= 20.96$  and its crystal size is 19.986nm. The second high peak at  $2\theta=24.51$  have high about 1319, the crystal size about 29.790 nm, and also it has a peak at  $2\theta= 24.00$  by its crystal sizes as 40.176 nm which perhaps they return peaks to factional groups for  $A_2$  in addition to the peaks of polymer nanoparticles [15].

As depicted in Figure S7, the obtained XRD diffractogram patterns of  $S_3$  have two high peaks which reach to 5330, the first at  $2\theta = 21.450$  that peaks at  $2\theta =20.53$  and the second peak which is smaller, reaches to 1628 at  $2\theta =24.49$  and it peaks at  $2\theta =23.96$ . The crystal size of the former sets at 26.944, 20.944, 28.726, and 40.176 nm, respectively. According to the literature, the shape of the first and the most intense peak reflects the ordered packing of the polymer chain [16].

#### Scanning Electron Microscope of Polymer Nanoparticle

SEM is considered as one of the most important techniques and it is used in investigating the

knowledge of morphology for the surface. It was studied for polymer acrylic, as depicted in Figure S18, which has a spherical shape and the diameters as 3.164, 4.980, and 11.09  $\mu\text{m}$ , respectively.

As presented in Figure S19, the morphological analysis of  $S_1$  appears as a white area having a rough surface. Moreover, the analysis indicates that nano dimensions in image with its size as 100 nm were about 65.13, 17.76, 83.63, 134.8, 183.1, and 205.5 nm, while the image with  $1\mu\text{m}$  size was about 81.88, 96.76, 169.7, 223.3, 644.4 nm and 1.004  $\mu\text{m}$ .

In Figure S20, the SEM images for  $S_2$  demonstrate the roughness of surface and the growth of some particles. The image with its size as 100 nm, the nano dimensions were about 35.36, 73.73, 122.7, and 227.8 nm, but the image with it size as 200 nm has the nano dimensions about 52.10, 66.99, 145.2, 179.9, and 186.9 nm.

As depicted in Figure S12, the SEM images for sample  $S_3$  show the surface morphology exhibiting in a rough surface. It has nano-size areas as 26.05, 48.38, 53.38, 94.54, and 135.7 nm with its volume as 100 nm, on the other hand in the above-mentioned Figure, the volume 1  $\mu\text{m}$  has sizes as 89.32, 96.76, 163.8, 254.1, 583.9 nm, and 1.167  $\mu\text{m}$ .

**Table 1:** Polymer polyacrylic doping with different Schiff base syntheses

S	$S_1$	$S_2$	$S_3$
Polymer	Polymer + $A_1$	Polymer + $A_2$	Polymer + $A_3$

**Table 2:** FT-IR absorption bands of ( $A_1 - A_3$ )

No.	$A_1$	$A_2$	$A_3$
N-H	3187	3357	3079
H-N-H	----	3180-3157	3002- 2962
C-H Aro.	2985-2906	2957	2929
C-H Alif.	2872	----	2839
N-C=O	1655 \ O-C=O 1751	1686	1598
C=N	1600	1657	1623
C=C Aro.	1498-1463	1604-1551	1579-1508
C-N	1369	1336	1362
C-O	1336	1352	1346

**Table 3:**  $^1\text{H-NMR}$  of ( $A_1 - A_3$ )

No.	$A_1$	$A_2$	$A_3$
-NH <sub>2</sub>	----	10.70, 10.52	7.08, 7.06
-NH	11.04	9.59	---
C-H Aro.	8.06- 6.29	7.36-6.84	7.49-7.38
N=C-H	---	----	8.64
C-H Alif	4.31 OCH <sub>2</sub> , 1.33 CH <sub>3</sub>	----	3.82, 3.35

**Table 4:**  $^{13}\text{C}$ -NMR of (A<sub>1</sub> – A<sub>3</sub>)

No.	A <sub>1</sub>	A <sub>2</sub>	A <sub>3</sub>
O-C=O	165.37	----	----
N-C=O	163.22	162.78	----
N=C	155.13	138.64	160.87
C=C Aro.	154.88- 111.69	127.06-109.99	151.60-108.96
O-CH	60.74	----	55.66, 55.42
C-H Alif	14.26	----	----

**Table 5:** FT-IR absorption bands of (S – S<sub>4</sub>)

No.	N-H	C-H Aro.	=C-H	C-H Alif.	C=O ester	C=O amid	C=N	C=C	C-N	C-O
S	---	---	3002-2963	2930-2837	1622	----	---	1590-1508	1344	---
S <sub>1</sub>	3400	3017	2946	2918-2849	1730	1162	1604	1590	1247	1243
S <sub>2</sub>	3400	3014	2918	2849	1733	1690	1590	1482	1272 N-N 1467	1194
S <sub>3</sub>	3400	3012	2919	2849	1730	----	1620	1482	1273 N-N 1467	1242 C-O <sub>ether</sub> 1270

**Table 6:** XRD data for prepared polymer and polymer nanoparticles doping with some Schiff base compounds

No.	2 $\theta$	High	FWHM	Crystal Size (D)
S	13.2	592	2	3.956
	30.9	139	7	1.165
	42.7	70	4	2.110
S <sub>1</sub>	5.38	831	0.17	46.319
	6.85	875	0.27	29.163
	20.47	1177	0.31	25.762
	21.467	7360	0.204	39.224
	23.67	683	0.19	42.290
	24.01	1268	0.23	34.935
	24.01	2331	0.22	36.561
S <sub>2</sub>	5.30	557	0.21	37.496
	6.78	606	0.4	19.685
	20.96	937	0.4	19.986
	21.459	4990	0.24	33.343
	24.00	969	0.24	40.176
S <sub>3</sub>	24.51	1319	0.27	29.790
	6.83	912	0.38	20.721
	17.07	518	0.4	19.884
	20.53	750	0.39	20.98
	21.450	5330	0.297	26.944
	24.49	1628	0.28	28.726
25.70	506	0.34	23.730	

## Conclusion

The results of the study confirmed the characterization of the polymer polyacrylic nanoparticles which were prepared by emulsion method in nano sizes. Then after, the crystallite sizes of the sample were calculated using the

Scherrer formula which was in the range of up to the nano sizes as 17-50 nm. The particle size was considered based on the SEM surface morphology of nanoparticles. With high-resolution images of the sample, these images gave the irregular and

angular shapes with different particle sizes and different diameters in the range of 20-600 nm.

This research reported the study of a series of Schiff base syntheses from Isatin with different aromatic amines for two Schiff base preparations A<sub>1</sub>, A<sub>2</sub> and A<sub>3</sub> synthesis from 3,4-dimethoxy benzylidene with Hydrazine. The physical characterization using spectroscopic techniques was employed in the elucidation of the structures of the synthesized derivatives which indicated the analysis through spectrum IR, <sup>1</sup>H- NMR, and <sup>13</sup>C-NMR to the structures of these compounds.

### Funding

This research did not receive any specific grant from funding agencies in the public, commercial, or not-for-profit sectors.

### Authors' contributions

All authors contributed toward data analysis, drafting and revising the paper and agreed to responsible for all the aspects of this work.

### Conflict of Interest

We have no conflicts of interest to disclose.

### ORCID:

Soraj A. Rahem

<https://www.orcid.org/0000-0002-9287-915X>

### References

- [1]. Badawi A.A., Nour S.A., Sakran W.S., Shereen Mohamed Sameh El-Mancy; *AAPS PharmSciTech*, 2009, **10**:4 [Crossref], [Google Scholar], [Publisher]
- [2]. Yadav V., Jadhav P., Kanase K., Bodhe A., Dombé S., *Int. J. Appl. Pharm.*, 2018, **10**:138 [Google Scholar]
- [3]. Fickert J., *Nanocapsules for self-healing materials* (Doctoral dissertation, Johannes

Gutenberg-Universität Mainz). 2013 [Google Scholar]

- [4]. Sane R., Mittapalli R.K., Elmquist W.F., *J. Pharm Sci.*, 2013, **102**:1343 [Crossref], [Google Scholar], [Publisher]
- [5]. Salerno C., Gorzalczy S., Arechavala A., Scioscia S.L., Carlucci A.M., Bregni C., *Rev. Colombia Sci. Quim. Farm.*, 2015, **44**:359 [Crossref], [Google Scholar], [Publisher]
- [6]. Winey K.I., Vaia R.A., *MRS bulletin*, 2007, **32**:314 [Crossref], [Google Scholar], [Publisher]
- [7]. Shiju C., Arish D., Bhuvanesh N., Kumaresan S., *Spectrochim. Acta A Mol. Biomol. Spectrosc.*, 2015, **145**:213 [Crossref], [Google Scholar], [Publisher]
- [8]. Omidi S., Kakanejadifard A., *RSC Adv.*, 2020, **10**:30186 [Crossref], [Google Scholar], [Publisher]
- [9]. Al Zoubi W., *J. Coord. Chem.*, 2013, **66**:2264 [Crossref], [Google Scholar], [Publisher]
- [10]. Da Silva C.M., da Silva D.L., Modolo L.V., Alves R.B., de Resende M.A., Martins C.V., de Fátima Â., *J. Adv. Res.*, 2011, **2**:1 [Crossref], [Google Scholar], [Publisher]
- [11]. Lima E.C.D., Souza, C.C.D., Soares R.D.O., Vaz, B.G., Eberlin M.N., Dias A.G., Costa P.R., *J. Braz. Chem. Soc.*, 2011, **22**:2186 [Crossref], [Google Scholar], [Publisher]
- [12]. Joothamongkon J., Asawapirom U., Thiramanas R., Jangpatarapongsa K., Polpanich D., *RSC Adv.*, 2020, **10**:33279 [Crossref], [Google Scholar], [Publisher]
- [13]. Koseoglu B., *Izmir Inst. Technol.*, 2011 [Google Scholar], [Publisher]
- [14]. Zhang M., Zhang S., Chen Z., Wang M., Cao J., Wang R., *Polymers*, 2019, **11**:1891 [Crossref], [Google Scholar], [Publisher]
- [15]. Todica M., Stefan T., Simon S., Balasz I., DARABAN L., *Turk. J. Phys.*, 2014, **38**:261 [Google Scholar]
- [16]. Gultek A., Seckin T., Onal Y., Icduygu M.G., *Turk J. Chem.*, 2002, **26**:925 [Google Scholar]

### HOW TO CITE THIS ARTICLE

Mohsin E. Aldokheily, Athraa H. Mekky, Soraj A. Rahem. Preparation of Polymer Nanoparticles and Doping by Some Schiff Base Compounds by using Microemulsion Systems. *Chem. Methodol.*, 2022, 6(6) 494-500

<https://doi.org/10.22034/CHEMM.2022.334829.1459>

URL: [http://www.chemmethod.com/article\\_148574.html](http://www.chemmethod.com/article_148574.html)